



# Back calculation and hazard prediction of a debris flow in Wenchuan meizoseismal area, China

Bo Liu<sup>1</sup> · Xiewen Hu<sup>1</sup> · Guotao Ma<sup>1,2</sup>  · Kun He<sup>1</sup> · Mingyan Wu<sup>3</sup> · Dingyi Liu<sup>1</sup>

Received: 19 August 2020 / Accepted: 2 February 2021 / Published online: 22 February 2021  
© Springer-Verlag GmbH Germany, part of Springer Nature 2021

## Abstract

On August 20, 2019, many catastrophic debris flows broke out in meizoseismal area of Wenchuan M s 8.0 earthquake in China under the influence of continuous heavy rainfall. This paper takes the Chutou gully debris flow event occurred on August 20, 2019 as an example. The 3-D numerical simulation software, RAMMS, is used to back calculate the event and predict the future hazard. Coulomb and viscous turbulent friction,  $\mu$  and  $\xi$  are calibrated in RAMMS. Numerical simulation reveals the movement process of Chutou gully from the aspects of flow depth, velocity, discharge, and run-out solid materials volume. The simulation results show that more than two-thirds of the solid materials are still deposited in the main channel, which could provide material basis for the re-occurrence of high hazard debris flow. In addition, based on the intensity and probability of debris flow, the hazard of debris flow is divided into high, middle, and low degrees. According to the simulation results and hazard assessment model, the hazard map of Chutou gully debris flow in various rainstorm return periods (20, 50, 100, and 200 years) is established, which can provide guidance for the future land-use planning and debris flow prevention works.

**Keywords** Debris flow · RAMMS · Numerical simulation · Voellmy · Salm · Back calculation · Hazard prediction

## Introduction

Since the devastating earthquake in Wenchuan on May 12, 2008, the main type of geological hazard has gradually transformed into debris flow from collapse and landslide in such meizoseismal area because that earthquake induced collapses increased the volume of loose material in gullies (Huang and Li 2009). After this, heavy rainfall-induced debris flows hit severely earthquake-stricken zones, causing casualties and destruction of housing, bridges, and transport facilities. Several researches suggested the impact by earthquake may retain up to 20 years (Lin et al. 2004; Chang et al. 2009; Fan et al. 2019a). According to some literature, post-earthquake debris flows are induced by extremely heavy rainfall with synergy

between various factors including steep topography, surface, and gully erosion. In post-earthquake period, rainfall threshold of debris flow begins with a remarkable drop and then goes back continuously (Guo et al. 2016; Ma et al. 2017; Penserini et al. 2017). Gullies in meizoseismal area store an immense amount of landslide accumulation, which provides adequate sources and contributes to promoting debris flow scale (Ge et al. 2015; Fan et al. 2019b). In situ investigation, however, is still a typical way to acquire first-hand data, with lots of manpower, time, and low efficiency (Luo et al. 2017; He et al. 2021). Given the difficulty of model experiments and field observations, the combined numerical simulation and in situ investigation have become a significant approach in debris flow study (Wang et al. 2018).

As such a series of processes which is between block movement (e.g., collapse and landslide) and sand-containing waterflow, debris flow forms by interaction between solid and liquid phase in channels and moves with different velocities in different flow height causing shear stress by interlayer friction. In terms of its complexity, hardly does one model reflect perfectly features of debris flow. Numerical approaches have been proposed that are not based on the construction of meshes (structured or unstructured) which have proved effective for the study of muddy debris flow, i.e., mesh-less

✉ Guotao Ma  
maguotao46@yahoo.com

<sup>1</sup> Faculty of Geosciences and Environmental Engineering, Southwest Jiaotong University, Chengdu 611756, China

<sup>2</sup> School of Engineering, University of Warwick, Coventry CV4 7AL, UK

<sup>3</sup> School of Resources and Safety Engineering, Chongqing University, Chongqing 400044, China

approaches represented by SPH (smoothed particle hydrodynamics) (Pastor et al. 2014; Minatti and Pasculli 2011). However, SPH requires a certain number of numerical particles to assure the accuracy and computational stability because of the inherent discontinuity problem at the boundaries. Therefore, continuum models such as Voellmy, Bingham, and Coulomb model are often utilized to depict such non-Newtonian fluid's properties. Rickenmann et al. (2006) found that although models above stated have a good congruence on the flow range of debris flow, the Bingham model may produce a more rapid velocity, and the friction of the basement has a greater impact on the deposition. Naef et al. (2006) compared the effects of eight different combinations of rheological resistance relationships including Bingham, Voellmy, and Turbulent and Coulomb on the numerical calculation of debris flow, and concluded that the resistance relationship with turbulent had the best results. Various geological conditions conduct various models (Bertolo and Bottino 2008). In the analysis of Medina et al. (2008), the Voellmy model shows the best in both flow characteristics and deposition characteristics regarding comparison of flow damping between models of Bingham, Herschel-Bulkley, and Voellmy. With respect to debris flows in meizoseismal area, both Wu et al. (2015) and Horton et al. (2019) found that turbulence coefficient value, in Voellmy model, was bigger than actual so that to produce a more reasonable result of run-out coverage prediction. Rapid mass movements simulation (RAMMS) is a debris flow numerical simulation software, adopting refined Voellmy–Salm model in which turbulence coefficient is added to be in line with real condition, based on geographic information system (GIS) (Gan and Zhang 2019). Compared to Flo-2d, another similar software but fail to consider the interaction between fluid and down bedding, RAMMS need no pre-definition of migration pathway and is capable of considering the impact of gully erosion through built-in empirical model (Huang et al. 2009). Moreover, RAMMS is allowed to set inflow according to the actual condition by block release or hydrological curve input which makes the initial inflow condition more consistent with actual, while other software (e.g., Massflow, DAN-W, and Flo-2d) is only allowed by either (Huang et al. 2014). Furthermore, RAMMS has a powerful 3D visualization function to calculate on the relief map and view the time-sharing results of the entire process.

Chutou gully was taken to discuss the application method of RAMMS for simulation and prediction. Firstly, RAMMS was used to simulate the initiation and following movement of debris flow occurred in Chutou gully on August 20, 2019 to determine friction coefficient in the refined Voellmy–Salm fluid model. Secondly, various factors of the whole process, including flow depth, velocity, and discharge were analyzed through monitor points setting in gully. Compared with field investigations, RAMMS was tested whether it did precise work. Finally, hazard classification standard was established

on the base of simulating intensity and flow depth of debris flow, and hazard map of Chutou gully under various rainfall return periods was made to guide for land utilization planning and prevention and control designing in post-earthquake rebuilding area.

## Backgrounds

### Geological setting

Research zone, located in Miansi Township in Wenchuan county of China's southwestern Sichuan province, is 30 km from the epicenter of M8.0 Wenchuan earthquake of May 12, 2008. According to Fig. 1, research zone is situated tectonically on Longmenshan fault zone and Yinxiu-Beichuan fault runs through the outlet of Chutou gully, endowing joints and fractures in a large-scale and deeply fractured rock mass (He et al. 2020; Yan et al. 2020). With elevation range from 1178 to 4130 m and leaf-like catchment area of 21.7 km<sup>2</sup>, incised V-shaped Chutou gully has an 8900-m long-main channel featured by inclination of 184‰, where more than 87% of the slopes angle over 20°. The mean slope inclination angles approximately 37°. The main lithology of this region is pre-Sinian granite, Silurian phyllite, Carboniferous limestone, and Triassic sandstone.

In Chutou gully, 16 branches are scattered, with down-cutting erosion in depth between 8 and 15 m, which are narrow, steep, and well-hydrodynamic (Fig. 2). Slope inclination of them ranging from 45° to 65° and certain are up to 80°. The inclination of branch lies in the range of 371 to 737‰ and the width of bottom is mostly from 10 to 16 m. What stated above provides adequate sources supply and dynamic condition for Chutou gully debris flow. After earthquake, a great deal of slumping mass has generated in Chutou gully, changing original landscape extremely. Ninety-three source areas were marked (Fig. 2) with dynamic reserve of  $336.07 \times 10^4 \text{ m}^3$  among total volume of  $1366.67 \times 10^4 \text{ m}^3$  in accordance with field investigation. The size of source is mainly concentrated from 0.05 to 0.5 m, fine-grained material increases, and coarse-grained material decreases from upstream to downstream along channels.

### Debris flow events

In Chutou gully, two debris flow events occurred. One was on July 10, 2013 and another was on August 20, 2019 (i.e., “7.10” debris flow and “8.20” debris flow respectively). Historical satellite imageries from different periods show the dynamic processes of depositional fan (Fig. 3). Before Wenchuan earthquake, Chutou gully kept its complete topography and covered by lush plants, none of public facilities on its outlet (Fig. 3a). Affected by the “5.12” Wenchuan

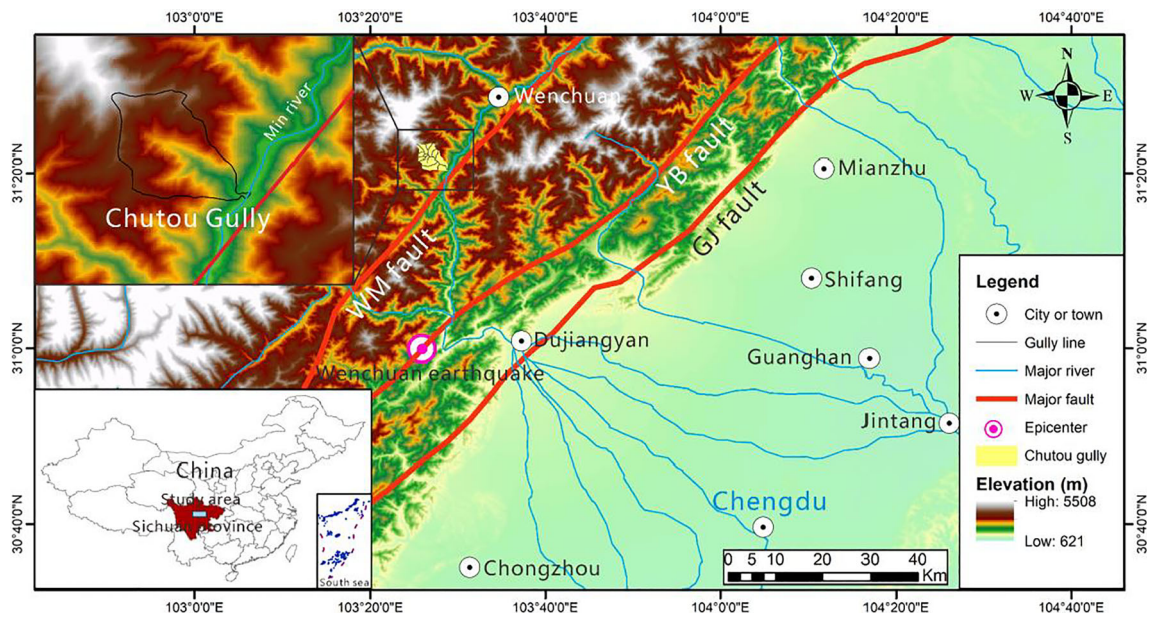


Fig. 1 Tectonic map. (WM is Wenchuan-Maoxian, YB is Yingxiu-Beichuan, and GJ is Guanxian-Jiangyou)

earthquake, topography was damaged severely, forming collapse, landslide source materials. In the reconstruction project, the local government have built motorway from Dujiangyan

to Wenchuan and widen the national way G213, both of which intersected the outlet of Chutou gully (Fig. 3b). On July 10, 2013, a massive debris flow rushed outlet and formed alluvia

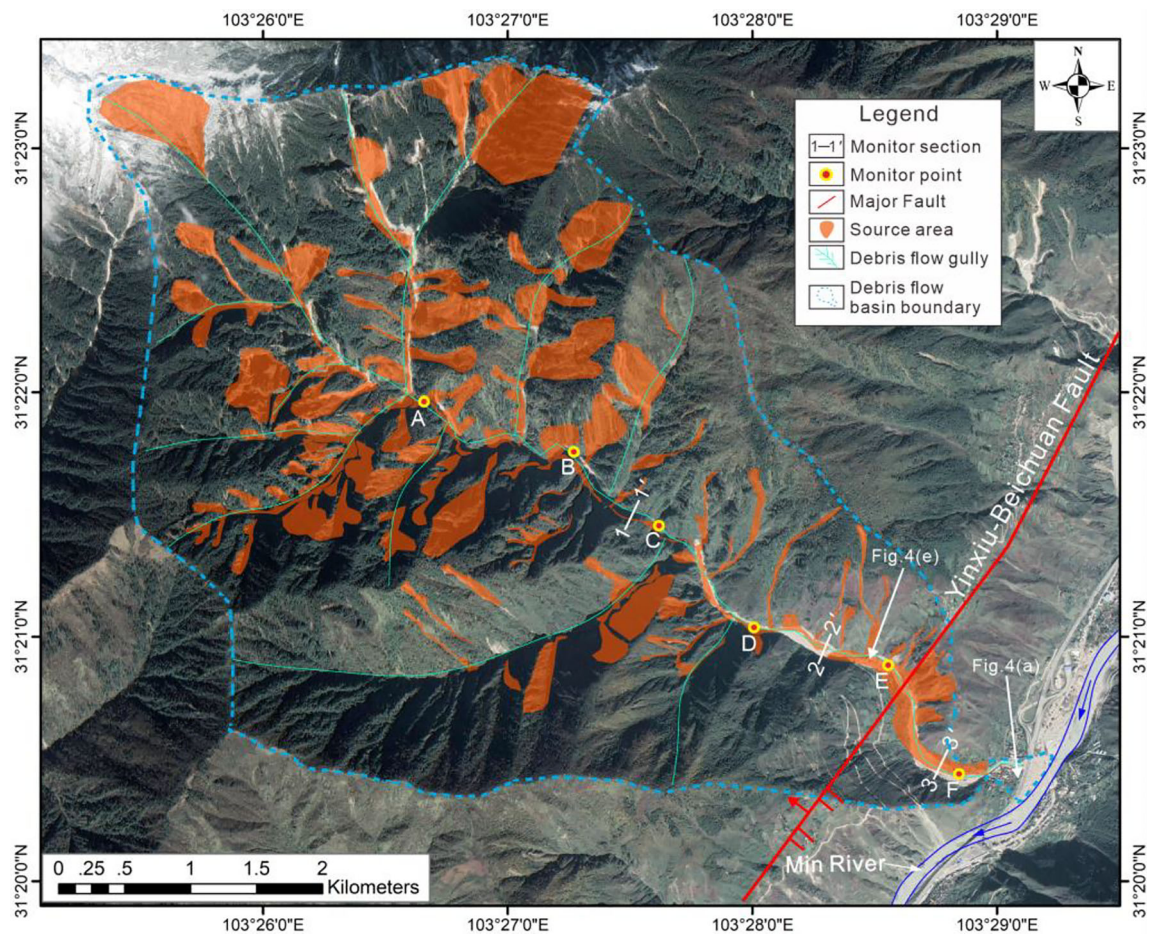
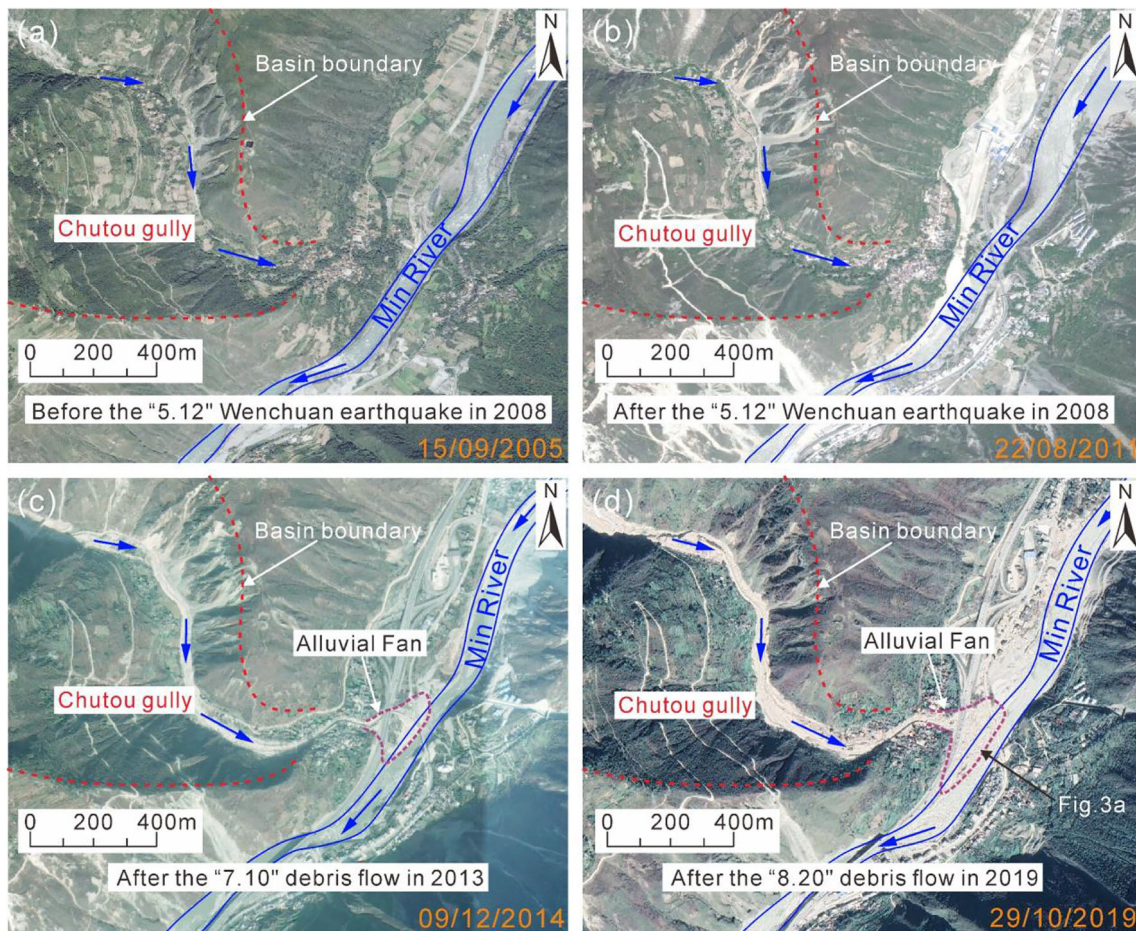


Fig. 2 Satellite imagery of Chutou gully with sources. (Based on Google satellite imagery at Nov 7, 2015)



**Fig. 3** Historical satellite imageries at different time. **a** Before the “5.12” Wenchuan earthquake in 2008. **b** After the “5.12” Wenchuan earthquake. **c** After the “7.10” debris flow. **d** After the “8.20” debris flow

fan (Fig. 3c). Then, the construction of retaining dams and drainage channels followed in accordance with 5% rainfall frequency. On August 20, 2019, another debris flow, being much larger than before, cascaded once again as a result of persistent torrential rain in Wenchuan (Figs. 3d and 4a). DEM differences between pre- (from ALOS) and post-debris flow

(using UAV) reveal that the deposits volume is about  $85.4 \times 10^4 \text{ m}^3$  (Fig. 4e). Prevention and control construction were destroyed totally and nearly 200-m-long section of highway passing outlet was buried. More horribly, the bridge of G231 over the Min River was broken (Fig. 4c) and more than 10 houses were damaged (Fig. 4d). Over half of the riverbed was



**Fig. 4** Features of Chutou gully on Aug 20, 2019. **a** Panorama of depositional fan; **b** destroyed houses in downstream; **c** broken bridge; **d** affected village; **e** Gorged dam with debris flow materials, the location is showed in Fig. 2.

blocked so that water spilled and was pushed to the opposite bank, making damage to the village (Fig. 4b). But fortunately, due to the timely notification of the evacuation by the government, no casualties were caused.

### Causes and formation

The formation conditions of post-seismic debris flow mainly include sources, topography and water, among which impact of sources and of water are particularly obvious. Usually, accumulated rainfall and rainfall intensity are so high when debris flows are ready to commencement (Crosta 1998). Previous research (Li et al. 2016) reported a recorded rainfall that induced debris flow in southwestern China, accumulated rainfall nearly reaching 100 mm. The rainfall amount of Miansi town causing “8.20” debris flow is showed in Fig. 5 based on the observation data records of Yangdian Meteorological Observation Station. The rainfall started on August 18, 2019, and mainly concentrated on 19th and 20th. The outburst of debris flow in Chutou gully was at 2:00 AM on August 20. Until the outbreak of debris flow, the accumulated rainfall and critical rainfall intensity were 148.1 mm and 18.6 mm/h respectively.

Though difficulties stand the front of precise prediction of rainfall threshold inducing debris flows in meizoseismal area, Fan et al. (2019a) established an early-warning model of intensity duration (I-D model) of rain-induced debris flow in Wenchuan, through analyzing of debris flows and rainfall data from 2008 to 2013, on the base of post-seismic debris flows database of Wenchuan. In I-D model, the dotted line is the fitting line of the rainfall threshold of debris flow, above which is debris flow occurrence area meaning high occurrence probability of debris flow. As illustrated in Fig. 6, the rainfall duration before the event was about 52 h, and the average rainfall per hour was 2.85 mm, which was far over the threshold (drawn by dotted line). According to the pre-seismic data, early accumulated rainfall of Wenchuan was between 320 and 350 mm while the critical rainfall intensity was between 55 and 60 mm/h (Fan et al. 2019b). The early accumulated rainfall and hourly average rainfall of “8.20” debris flow is merely 127.85 mm and 24.37 mm, both of which were 1/3 to 1/2 of

**Fig. 5** Hourly rainfall amount and accumulated rainfall before and after the “8.20” debris flow in Chutou gully

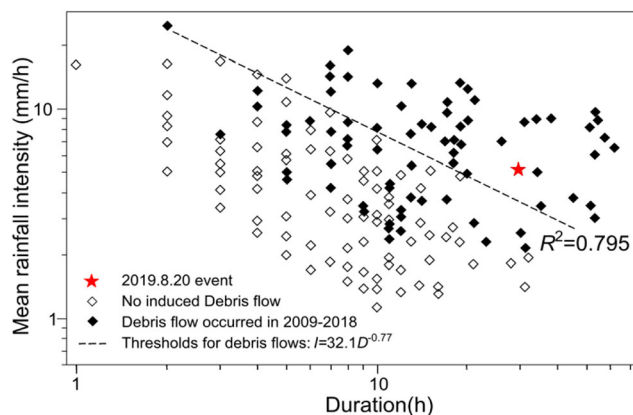
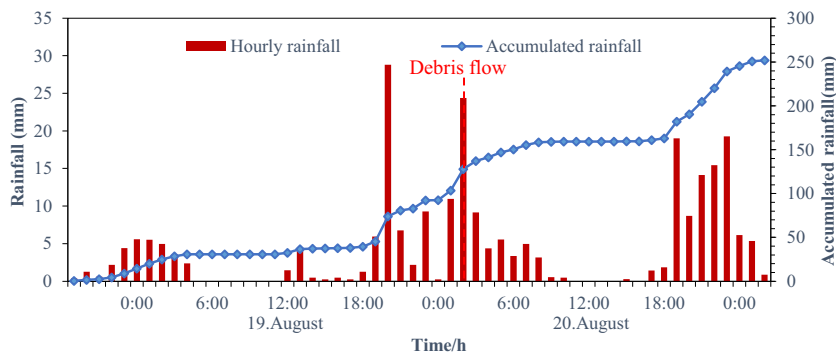


**Fig. 6** I-D model of Chutou gully (Quoted from Fan et al. (2019a), with changes)

those in pre-earthquake period, indicating the long-term impact of Wenchuan earthquake on meizoseismal area.

The development characteristics of debris flow sources in meizoseismal area are mainly controlled by topography and earthquake, but also influenced by erosion and transportation in rainy season (Fan et al. 2019b). After the earthquake, the upper bedrock (or surface) of the collapsed body is exposed, significantly strengthening catchment’s capacity. With quick collection of water and taking loose materials, viscous torrents are forming and rapidly rushing into the channel. At the same time, during the movement of debris flow, multiple branches often erupt simultaneously, continuously providing sources to main channel. Therefore, the flow increasing flow eventually morphs into a fatal debris flow (Fig. 4a).

In short, the trigger of the debris flow in Chutou gully may be continuous heavy rainfall. At the same time, sufficient sources in channels are responsible for the huge amount of run-out material.

### Method

#### Analysis procedure

The analysis process is shown in Fig. 7. Firstly, to provide input data of database for disaster analysis, basic data are

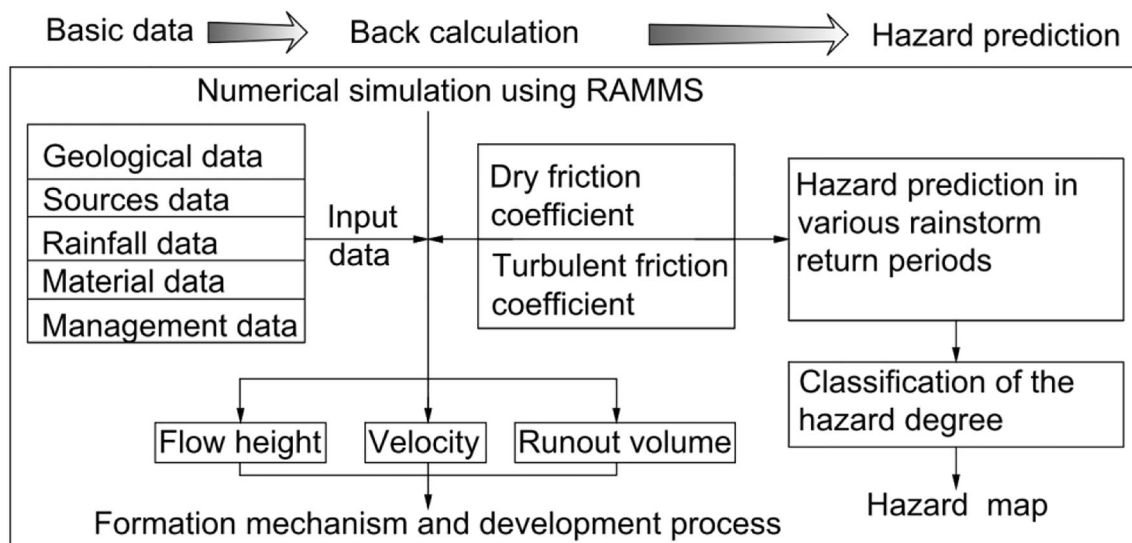


Fig. 7 Flow diagram to analysis

collected (topography, hydrological condition, sources, etc.) through the field investigation and remote sensing interpretation. Then, research zone is divided into a grid, each part is assigned attributes including area, elevation, inclination and soil property. The five types of input data are shown in Fig. 7, namely geological, sources, rainfall, materials and management data. (Geological data involve digital topography, aerial and satellite images with geographic coordinates and maps with more information, which is mainly used to construct a fundamental 3D map for further debris flow simulation. Source data cover the location and volume, which can be used to define the starting conditions of debris flow by block release method. Rainfall data include data from the past few years and on-site monitoring, which are useful to analyze rainfall patterns, the space-time distribution characteristics of local rainfall, and early or key rainfall in past important events. Materials data mainly consist of outdoor and indoor experimental data of basic physical and mechanical properties of soil and rock, which are capable of simulation of fluid characteristics of debris flow. Management data comprise detailed disaster history, existing disaster mitigation measures, on-site investigation of major disasters and affected entities, and is mainly used to determine sources and verify simulation results.) And lastly, a geographic information system (GIS) database for each data type is built via the GIS platform.

In process of database construction, geological data are usually spilt into vector-type data (such as calculation range) and grid-type data (for example digital elevation model (DEM) and satellite images). The latter can be classified using the GIS platform. The rainfall, materials and management data are usually in the form of tables or texts, which are classified into corresponding directories or folders according to attributes.

RAMMS provides block release and input hydrograph to define initial conditions of debris flow. These two ways should be chosen in consistence of detail of acquired data (Christen et al. 2010). Hu et al. (2014) proposed that deposition formed by Wenchuan earthquake should be deemed potential sources totally. For the “8.20” debris flow, the location and volume of slope failures and increased channel siltation should be confirmed by field investigation and remote sensing satellite images (Fig. 2), resulting in block release was selected. Then, given the location and volume of sources that cannot be figured precisely, a starting condition should be defined with input hydrography. Hydrographic charts were also used and calculated by the *Sichuan Basin Flood Calculation Manual* (Shen et al. 1984). At last, fluid parameters and terrain should be calibrated and be updated in terms of previous events.

To gain better simulation, the friction coefficients of Chutou gully can be acquired from back calculation. Then, results including flow depth, velocity and run-out material volume should be verified by actual situation. Following above, hazard classification standard was established, and hazard map of Chutou gully was made under various rainfall frequencies.

### Voellmy–Salm fluid model

Let  $X$  and  $Y$  be horizontal coordinates in a fixed Cartesian coordinate system and  $Z(X, Y)$  denote a mountain profile parameterized in  $X$  and  $Y$ . The independent variables  $x$  and  $y$  denote the arc length along the surface topography, the  $z$ -coordinate is perpendicular to the profile (Fig. 8). The coordinates  $x$ ,  $y$ , and  $z$  define the surface induced coordinate system. Its orientation varies with the position on the surface, such that

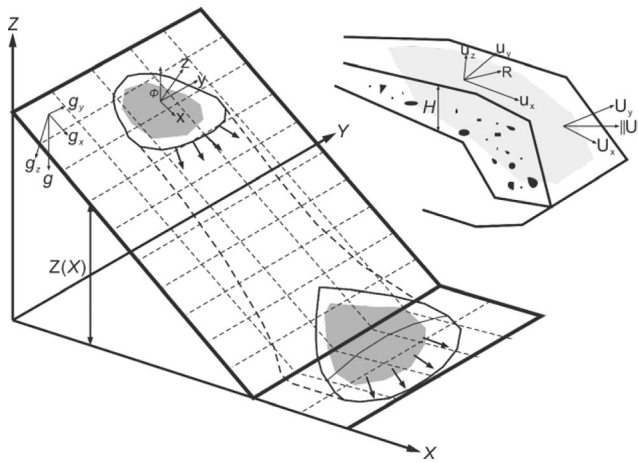


**Fig. 8** The topography  $Z(X, Y)$  is given in a Cartesian framework,  $X$  and  $Y$  being the horizontal coordinates. The surface induces a local coordinate system  $x, y, z$ . It is discretized such that its projection onto the  $X, Y$  plane results in a structured mesh

the vector of gravitational acceleration  $g = (g_x, g_y, g_z)$  has three non-zero components in general, in each case functions of  $x$  and  $y$ . Time  $t$  completes the set of independent variables for the system.

RAMMS adopts Voellmy–Salm fluid model, a continuum model, to show flow characteristics, in which debris flow is assumed to unstable and heterogeneous fluid depicted by fluid height  $(H(x, y, z)(m))$  and mean velocity  $(U(x, y, t)(m/s))$  (Bartelt et al. 1999; Frank et al. 2017).

$$U(x, y, t) = [U_x(x, y, t), U_y(x, y, t)]^T \tag{1}$$

where  $U_x$  is the velocity in  $X$  direction,  $U_y$  is the velocity in  $Y$  direction and  $T$  is the denotation of transposed matrix of average velocity. Note that the velocity can be defined as follows:

$$\|U\| = \sqrt{U_x^2 + U_y^2} \tag{2}$$

where  $\|U\|$  is the modulus of the velocity and  $U$  shall be strictly positive in vector space, whose direction should be defined by unit vector as follows:

$$n_u = \frac{1}{\|U\|} (U_x, U_y)^T \tag{3}$$

The basic balance law should be a deduction from conservation of mass and the first principle of conservation of momentum. The geometry form showing debris flow’s feature of shallow-layer flow indicates that lower shallow-layer parameter defined by the ratio of fluid height to fluid length. It is such geometric property that proves the correction to use mean depth field variation to represent the equation of model. The flow balance equation is established by  $H$  as follows:

$$\partial_t H + \partial_x(HU_x) + \partial_y(HU_y) = \dot{Q}(x, y, t) \tag{4}$$

where  $H$  is the fluid height (m),  $\dot{Q}(x, y, t)$  is term denoting material source ( $kg/(m^2 \cdot s)$ ). When  $Q = 0$ , there is no deposition. In the  $X$  and  $Y$  directions, balance equation of mean fluid depth should be described respectively:

$$\partial_t(HU_x) + \partial_x\left(c_x HU_x^2 + g_z k_{a/p} \frac{H^2}{2}\right) + \partial_y(HU_x U_y) = S_{gx} - S_{fx} \tag{5}$$

$$\partial_t(HU_y) + \partial_y\left(c_y HU_y^2 + g_z k_{a/p} \frac{H^2}{2}\right) + \partial_x(HU_x U_y) = S_{gy} - S_{fy} \tag{6}$$

where  $c_x$  and  $c_y$  are section coefficients,  $g_z$  is gravitational acceleration perpendicularly. In Voellmy–Salm model, contact relation in perpendicular aspect should be defined as anisotropic relation of Mohr–Coulomb (Savage and Hutter 1989; Bartelt et al. 1999; Pudasaini and Hutter 2007), in which positive stress in vertical (and horizontal) aspect varies in proportion to earth pressure coefficient ( $k_{a/p}$ ):

$$k_{a/p} = \tan\left[45^\circ \pm \frac{\phi}{2}\right] \tag{7}$$

where  $\phi$  is the internal friction angle of the debris flow. A large value of  $k_p$ , under the slow flowing condition, can induce a smaller  $H$  in run-out area. The right sides of the Eqs. (5) and (6) sum to the effective acceleration. The terms:

$$S_{gx} = g_x H \text{ and } S_{gy} = g_y H \tag{8}$$

where  $g_x$  and  $g_y$  are gravitational accelerations in  $X$  and  $Y$  direction respectively. Frictional resistance is divided, in Voellmy–Salm model, into the static frictional resistance including dry-Coulomb friction coefficient ( $\mu$ ), and the kinetic frictional resistance which related to velocity and viscous-turbulent friction coefficient ( $\xi$ ). Friction force  $S_f = (S_{fx}, S_{fy})^T$  is given as follows in Voellmy–Salm model:

$$S_{fx} = n_{U_x} \left[ \mu g_z H + \frac{g \|U\|^2}{\xi} \right] \tag{9}$$

$$S_{fy} = n_{U_y} \left[ \mu g_z H + \frac{g \|U\|^2}{\xi} \right] \tag{10}$$

where  $n_{U_x}$  is the velocity directional unit vectors in  $x$  direction, and  $n_{U_y}$  is the velocity directional unit vectors in  $y$  direction. Then total friction is separated into velocity-independent part and velocity-dependent part. The basic assumption of Voellmy–Salm model is that of shear deformations are gathered near the basal flow surface. The total friction force is as follows:

$$S = \mu \rho H g \cos(\phi) + \frac{\rho g U^2}{\xi} \quad (11)$$

where  $\rho$  is the mass density,  $g$  is the gravitational acceleration,  $U$  is the compounded velocity ( $U = (U_x + U_y)^T$ ).  $\rho H g \cos(\phi)$  is the normal stress on the overflowed surface.

The resistance force of solid phase ( $\mu$  denotes tangent of interior shear angle) and of viscous or turbulent phase ( $\xi$  is showed by hydrodynamic factor) were considered in Voellmy–Salm fluid model, Friction coefficients  $\mu$  and  $\xi$ , which are constant given by user, determine the flow properties of debris flow in RAMMS.  $\xi$  is dominant when debris flow in quick flowing state and  $\mu$  is dominant when debris flow in almost static state.

Many materials, like mud and snow, do not exhibit a simple linear relation ( $\mu = \text{constant}$ ) (Bartelt et al. 2017). Original Voellmy–Salm model can be revised as yield stress (i.e., cohesion). To simulate yield stress,  $N_0$  is introduced that gaining an ideal plastic material. In this case,  $N_0$  equals to a yield stress and  $\mu$  a “hardening” parameter. Then, neo-equation of frictional resistance is as follows:

$$S = \mu N + \frac{\rho g U^2}{\xi} + (1-\mu)N_0 - (1-\mu)N_0 e^{-\frac{N}{N_0}} \quad (12)$$

where  $N_0$  is yield stress of the flowing material and  $N$  is equal to  $\rho H g \cos(\phi)$ . Unlike a standard Mohr–Coulomb type relation, this formula ensures that  $S \rightarrow 0$  when both  $N \rightarrow 0$  and  $U \rightarrow 0$ .

Yield stress  $N_0$  serves to increase the shear stress for higher normal pressures. At low normal pressures (small flow heights), the shear stress increases rapidly from  $S = 0$  to  $S = N_0$ . The slope of the ‘S vs. N’ relation remains  $\mu$ , when the normal pressures are large. If  $\mu = 0$ , it shows a visco-plastic behavior (Bartelt et al. 2017).

## RAMMS simulation

RAMMS could simulate Chutou gully debris flow based on Voellmy–Salm model. At the assumption of continuous distribution of debris flow in space without any gaps, its physical quantities like velocity and density are continuous functions of time and space, which satisfy conservation of mass, momentum and energy. Before the simulation, a total simulation time needs to be set. When the simulation reaches the given time, the calculation stops. After many tests, we find that the debris flow basically stops at 3600 s. Meanwhile, the duration is consistent with that recalled by local villagers.

## Release zone and debris source materials

Starting conditions were set by block release. It may difficult for some areas of debris flow gully to reach and investigate because of broad cover and rugged topography. Tang et al. (2011) found average thickness of deposit of 21 debris flow gullies was from 1.0 to 8.2 m through aerial photo and field investigation. To estimate the volume of source areas, remote sensing images and InSAR technology were used. Shown by Fig. 2, 93 source areas were marked and thickness of each was valued. In the area where we can reach, the volume and thickness of material sources are mainly obtained through field investigation, which is a more accurate method. However, in the areas where manpower cannot reach, we estimate the area according to the average thickness estimation method provided by Tang et al. (2011). The average thickness of sources was about 1.5 m, the maximum thickness reaching 6.5 m, and the total volume of material sources was  $336.07 \times 10^4 \text{m}^3$ . However, it is still a challenge to obtain deposit thickness from satellite imageries because steep slope of research zone restrains application of InSAR technology.

## DEM and satellite images

Topography data serves as the most important input data, resolution and accuracy of which largely affect the simulation results. The discretization of the continuum using mesh requires the optimization of the number of elements and their distribution. The more the number of DEM elements, the more accurate the simulation results are, but it also requires higher computational capacity and simulation time. Many researchers have tested the effect of DEM resolution, such as Stolz and Huggel (2008) used three generically different digital elevation models (DEM) with grid spacing of 25, 4, and 1 m in conjunction with the flow models. The evaluation of the DEM grid spacing shows that for each flow model the 25-m DEM can give an approximate estimation of the potential hazard zone. 4- and 1-m DEMs mostly confine the simulated debris flow to existing channels and are in accordance with observations of recent debris flow events. Zhang et al. (2018) considered the computational capacity and simulation time, a 10-m DEM were processed from the pre-seismic satellite image to supply accurate topographic information for simulating deposits and debris flows. As shown in Fig. 2, we have included the entire catchment in the selected calculation range. Therefore, after estimating the computational capacity of our computer, the 5-m precision DEM, which was taken by advance land observe satellite (ALOS) launched in Japan in January 2006 was used as basic topographic data for numerical simulation, and the pixel count of simulated area is 117,030. Satellite images used in this paper main by Google earth, which originally came from aerial images and historical images (0.5 m spatial resolution) by Keyhole.



## Friction parameters

What the main difficulty debris flow simulation meets is component diversity of debris flow, which has a great influence on the selection of friction parameters. If the model parameters can be priority calibrated, then use of easy modeling methods should well simulate general characteristics of debris flows required for numerical simulation (Naef et al. 2006). Debris flow can be modeled to fluid with single-phase model by RAMMS. A greater friction coefficient may lead to a shorter movement process due to debris flow movement under the shadow of  $\mu$  and  $\xi$ ; therefore, friction parameters should be tuned so as to match observed /anticipated flow characteristics. Those characteristics include cross-sectional analysis, flow path, deposition of material and estimation of total volume, among which cross-sectional analysis is the most important one obtained by heights of levees or heights of marks on constructions, estimation of velocity (splashing, super elevation). Besides, the total volume is another important reference.

In accordance with in situ observation, debris flow model can be calibrated through comparing velocity and flow height of the same area. Follow steps are used to find the most appropriate  $\mu$  and  $\xi$ . At first, valuing the initial  $\tan(\alpha) = \mu = 0.2$  ( $\alpha \approx 15^\circ$ ) ( $\alpha$  is slope angle of assumed depositional area), and  $\xi = 200\text{m/s}^2$ . Then, adjusting them (floating range:  $\mu = \pm 0.05$ ,  $\xi = \pm 10\text{m/s}^2$ ) to find initial best-fit values of  $\mu$  and  $\xi$ , both of which served as a base of further fine-tuning after comparison between initial simulation results and actual observation. Finally, in the case of a given total source amount, by matching the simulation results of with actual observation of the height and velocity of debris flow at specified position, the most appropriate  $\mu$  and  $\xi$  of Chutou gully ( $\mu = 0.225$ ,  $\xi = 180\text{m/s}^2$ ) were found and further applied amid simulation of movement process of “8.20” debris flow event where various parameters (deposit depth, velocity, discharge of typical sections and total run-out volume) were used to analyze the movement of Chutou gully debris flow. The parameters adopted in simulations are shown on Table 1.

**Table 1** The parameters adopted in simulations

Parameters	Value
Friction coefficient, $\mu$	0.225
Viscous coefficient, $\xi$ ( $\text{m/s}^2$ )	180
Mass density, $\rho$ ( $\text{kg/m}^3$ )	1750
Simulation time, $t$ (sec)	3600
Simulation grid resolution (m)	5.0
Release volume ( $\text{m}^3$ )	$336.07 \times 10^4$
Number of elements	117,030

## Flow heights, velocities and run-out volume

### Flow height

Illustrated in Fig. 9, about 600 s after the starting of the debris flow, the sources on the sides and solid materials closer to the main channel were gathering, forming multiple source concentration points with a maximum flow depth of 7.52 m (Fig. 9a). When it came to 1200s, most sources had piled from branches to the main channel, and junctions of upstream branches and the main channel were the richest. At this time, the flow height surged significantly and deposition started (Fig. 9b). At about 2400 s, no sources moved to the main channel but those in two upstream branches. Material-intensive area had shifted to the middle and lower reaches with maximum flow depth of 15.73 m in middle reaches. Meanwhile, debris flow was rushing out of outlet (Fig. 9c). The sources had completed deposition at 3600 s, most of which distributed in middle and lower reaches with maximum flow depth of 13.42 m. Run-out solid material formed a fan shape with depositional depth from 0 to 4 m (Fig. 9d).

In order to better compare the simulation results with actual investigation, six monitoring points (A to F, showed by Fig. 2) were set up to observe the changes of flow depth at different time, and comparing the final flow depth with actual results. As shown in Fig. 10, the flow depth decreased rapidly, due to the reduction of solid materials recharge, after a spike (Fig. 10a, b, c). At the same time, channels in the middle and lower reaches were recharged by intermittent sources from branches so that multiple peaks of deposit depth appeared (Fig. 10b, c). When  $t = 1200\text{s}$ , solid materials has reached points D, E (where a check dam placed upstream) and F (Fig. 10d, e, f). No sooner than did debris flow reaches downstream flat section than deposition began, causing accumulating deposit depth which was close to 12 m eventually. The flood peak debuted in outlet of gully at about 2000s whose maximum height downstream topped to 4.7 m due to block of dam (Fig. 10f). As a simulation result, the final flow depth at each point basically tallies with that from field investigation but is slightly larger, especially in the upstream. The reason may be that when investigation was going, part of loose debris flow sediment had been taken away by running water.

### Velocity and discharge

Researches on debris flow velocities at different time show that flow velocity is related to topography amid the starting stage of debris flows. Since block release method is used in simulation which causes similarity of source starting to landslide, the steeper the slope the greater the starting velocity. However, flow velocity shows a closer relation to inclination and width of channels in the flowing stage. As shown in Fig. 11, the solid material at each source areas were fully started

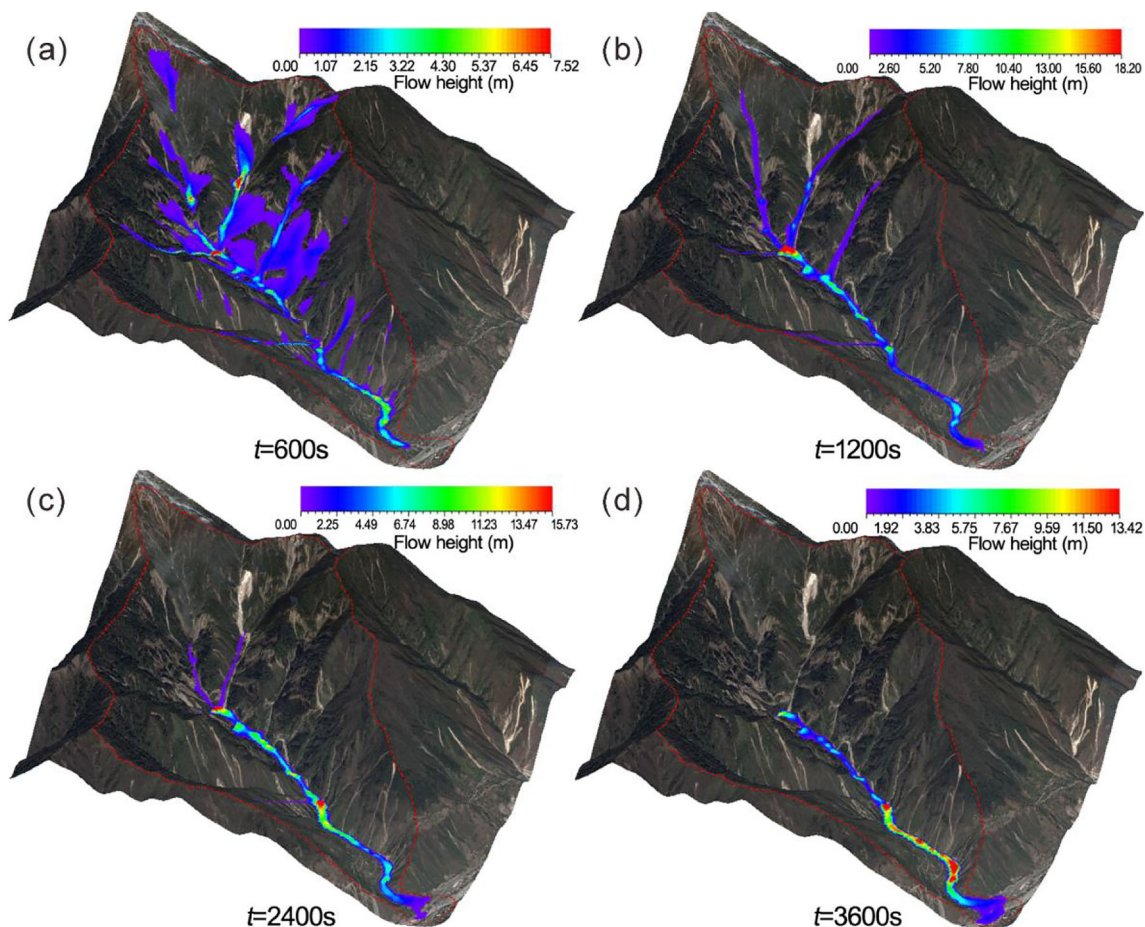


**Fig. 9** Characteristics of flow height when  $t = 600$  s (a), 1200 s (b), 2400 s (c) and 3600 s (d)

movement when  $t = 600$  s. Of them, the maximum velocity reached 14.96 m/s, which appeared at a shattered source point (Fig. 11a). When  $t = 1200$ s, the maximum velocity is 12.28 m/s of solid material which was in steep and narrow channel. In addition, the velocity in upstream main channel and branches is larger than that in downstream, indicating that solid material was swiftly gathering towards the main channel (Fig. 11b). As  $t = 2400$  s, the maximum velocity has shifted to middle and upper reaches resulted from narrow channel and extrusion effect (Fig. 11c), even though some solid material from branches was still moving to the main channel. After  $t = 3600$  s, the maximum velocity has transferred to the middle and lower areas because the confluence of branches was less than before. The velocity in outlet dropped to 2–5 m/s, which meant the development of debris flow has entered the deceleration accumulation stage accompanied with fan-shaped accumulation in outlet (Fig. 11d).

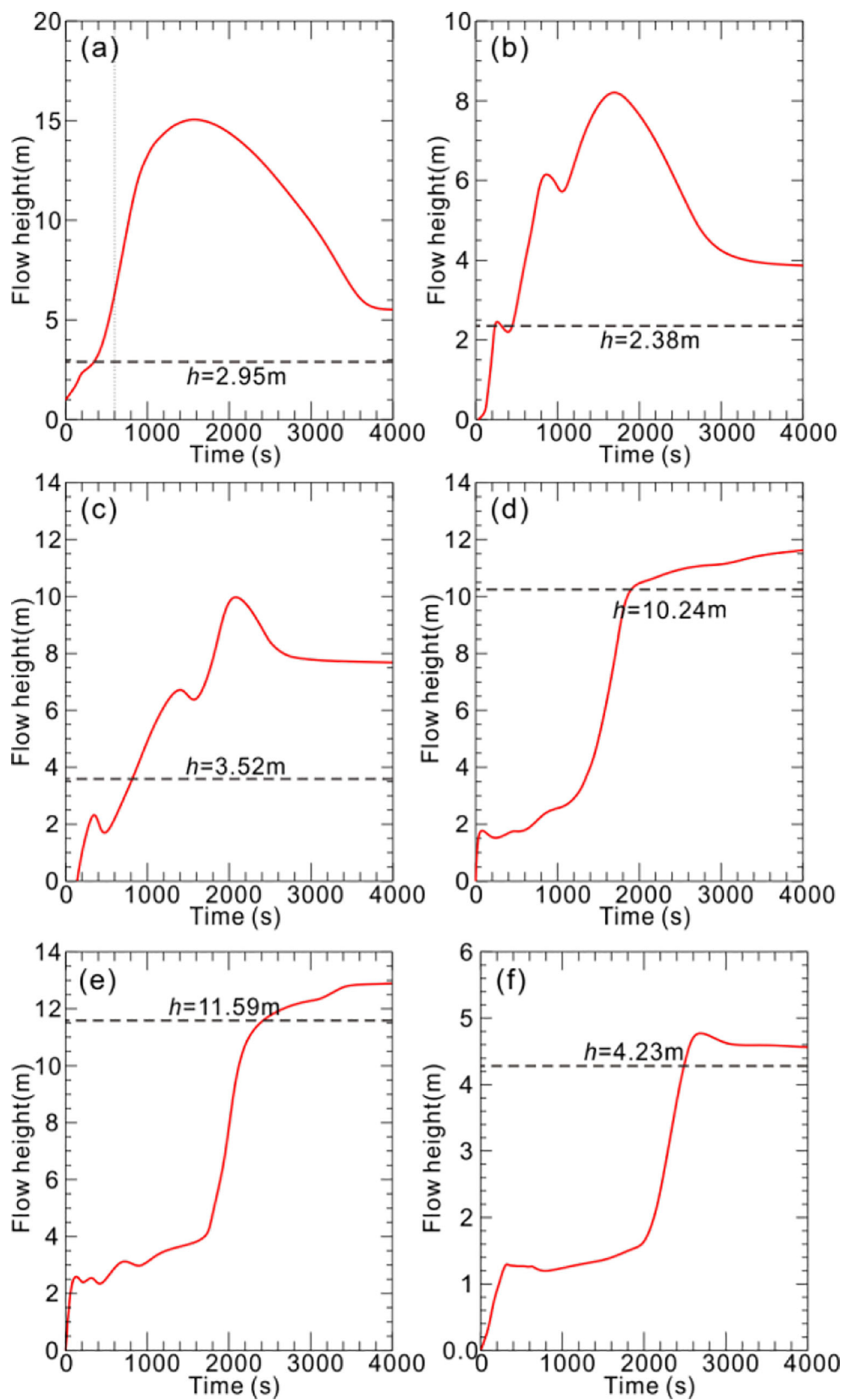
To figure out flow characteristics of debris flow, shown by Fig. 2 sections from upstream to downstream (1-1', 2-2', and 3-3') were introduced to monitor velocity and discharge. Figure 12 gives the flow characteristics at  $t = 600$  s, 1200 s, 2400 s, and 3600 s. With the movement of debris flow, in section 1-1', the velocity featured a hump shape. From 600

to 2400 s, discharge was increasing, up to a maximum of  $842.13\text{m}^3/\text{s}$ . When  $t = 3600$  s, debris flow entered the deposition stage with dropped discharge (Fig. 12a1–a4). In Section 2-2', the velocity feature was tantamount to that in section 1-1' but was less than 8 m/s. At 600 s, the discharge was less than that of section 1-1' but the maximum of  $955.52\text{m}^3/\text{s}$  was slightly larger considering material supplies from branches (Fig. 12b1–b4). In terms of section 3-3' near the outlet, both velocity and discharge were lower than those in section 2-2' due to deposition on a large scale (Fig. 9). The maximum discharge was only  $687.99\text{m}^3/\text{s}$  (Fig. 12c1–c4). The material rushed through section 3-3' and formed depositional fan outside the outlet, which may be one of reasons for river block, in Fig. 4, by debris flow considering annual mean discharge of  $452\text{m}^3/\text{s}$  of Min river (Tang et al. 2011).

#### Total run-out volume

The distribution of affected area, to a large extent, is influenced by the location of sources of debris flow and runoff characteristics. In practical applications, engineers and technicians often pay more attention to the range and volume of depositional fan that cause serious disasters (Prochaska et al.

**Fig. 10** Flow depth curves at different time in each monitoring point. **a, b, c, d, e** and **f** are the flow depth at monitoring point A, B, C, D, E and F, and the dashed line is the deposit depth measured in field investigation.



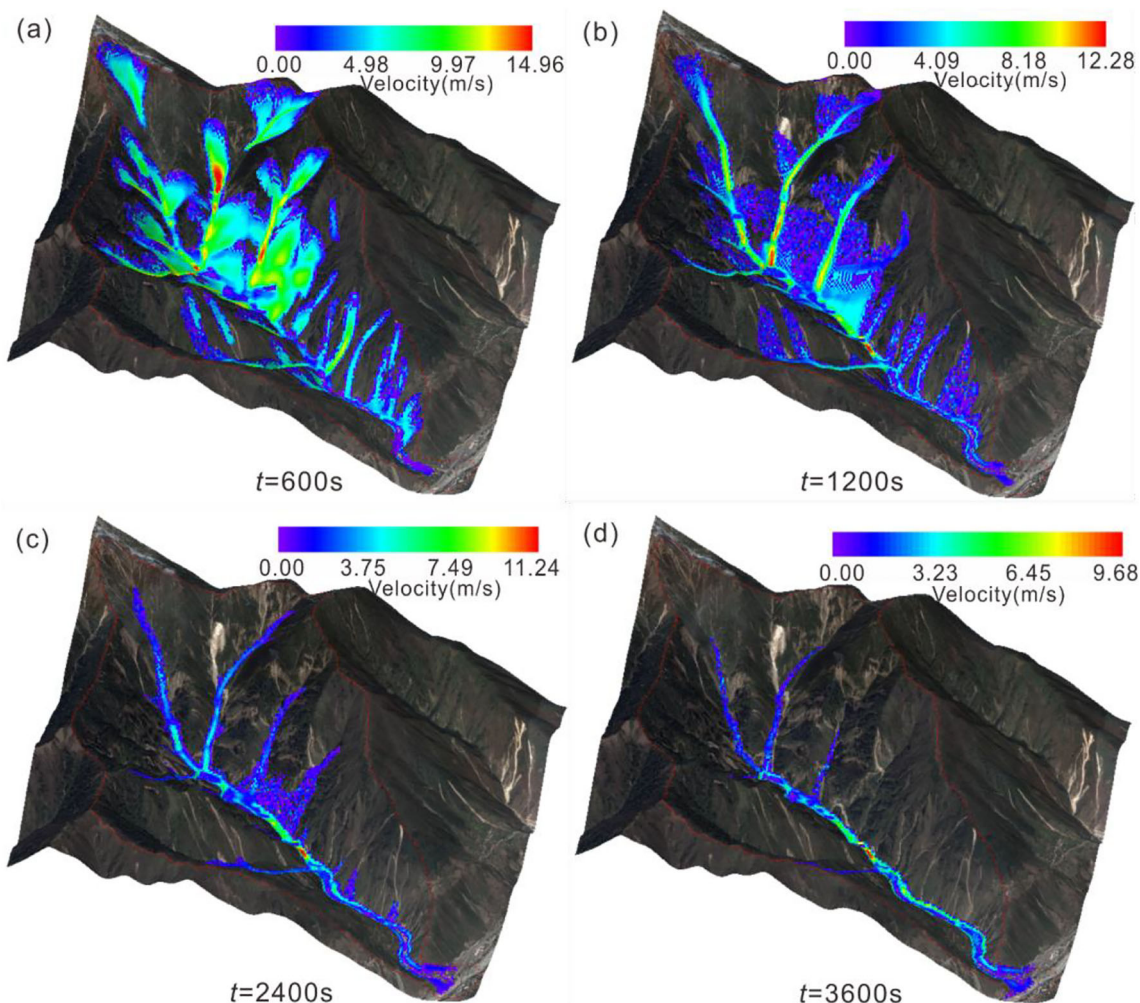


**Fig. 11** Characteristics of velocity when  $t = 600$  s (a),  $1200$  s (b),  $2400$  s (c),  $3600$  s (d)

2008). In this paper, the ASCII data of range and flow depth of depositional fan were acquired (Fig. 13), and total run-out volume was equal to the sum of the product of the flow depth and area of each pixel ( $5 \text{ m} \times 5 \text{ m}$ ) in the depositional fan. The calculation showed that the run-out volume of Chutou gully debris flow was about  $107.5 \times 10^4 \text{ m}^3$ , accounting for about 1/3 of the initial block release volume (Fig. 11d). This volume is larger than that observed which may be due to the fact that solid material that rushed into Min River could not keep its stay until discharge was great enough (Stolz and Huggel 2008).

## Hazard prediction

Input hydrograph was used to define starting condition of debris flow since different rainfall's induction of different starting material volume. This hazard map of Chutou gully under various rainfall return periods (20, 50, 100 and 200 years) was made on the base of hazard classification model.

## Hydrological curve

The hydrological map of these rainfall frequencies was obtained from the *Sichuan Basin Flood Calculation Manual* (Shen et al. 1984) and stated equations were used:

$$W_P = 0.1\psi H_{TP} F = 0.1HF \quad (13)$$

where  $W_P$  means flood volume of catchment ( $10^4 \text{ m}^3$ ),  $H_{TP}$  means total precipitation of catchment (mm),  $F$  means the catchment area ( $\text{m}^2$ ),  $\psi$  means surface runoff coefficient and  $H$  means channel runoff depth (cm).

$$Q_P = 0.278\psi i F = 0.278\psi (S/\tau^N) F \quad (14)$$

where  $Q_P$  is peak discharge in different return periods,  $i$  is rainfall mean intensity of rainfall (mm/h),  $S$  is rain force coefficient,  $\tau$  is convergence time of drainage,  $N$  is index of rainfall.

$$T_P = 2.78 (W_P/Q_P) \quad (15)$$

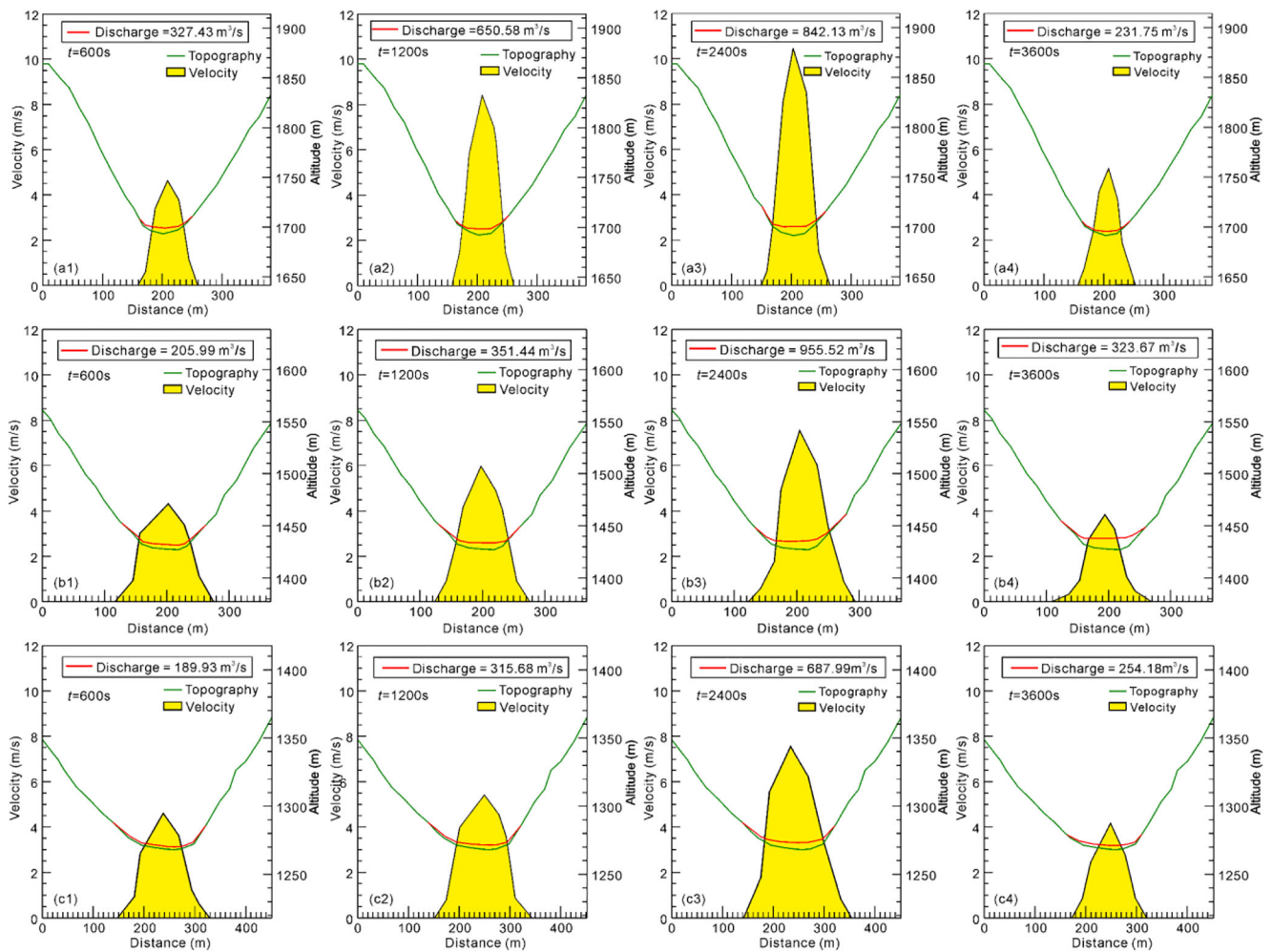


Fig. 12 Velocity and discharge of Chutou gully in section 1-1' (a1-a4), 2-2' (b1-b4) and 3-3' (c1-c4)

where  $T_p$  is flood duration in different return periods (h).

$$Q = yQ_p \tag{16}$$

$$T = xT_p \tag{17}$$

where  $Q$  is discharge ( $m^3/s$ ),  $T$  is debris flow duration (h),  $x$  and  $y$  are coefficients valued by *Sichuan Basin Flood Calculation Manual* (Shen et al. 1984) and bimodal curve was adopted. The hydrographic map (Return periods: 20, 50, 100 and 200 years), by equations (13) to (15), was shown in Fig. 14 where peak charges were 606.17, 814.02, 1168.75 and 1258.67  $m^3/s$ . It is indicated that the rainfall return period of the “8.20” debris flow was between 50 and 100 years.

### Hazard prediction map

This paper was based on the debris flow hazard classification of Fiebigler (1997) in Switzerland and Austria and Lin et al. (2011) in Taiwan. The debris flow intensity and occurrence probability were used to construct hazard map of debris flow,

and the probability of annual occurrence based on corresponding rainfall frequency can be calculated by Eq. (18) where  $n = 1$  (Lin et al. 2011).

$$P_n = 1 - \left(1 - \frac{1}{T}\right)^n \tag{18}$$

where  $P$  is the probability of annual occurrence based on corresponding rainfall frequency,  $T$  is recurrence period of debris flow and  $n$  is annual occurrence probability.

With reference to the hazard classification of debris flow in Taiwan (Lin et al. 2011), the occurrence probability adopted the following classification: Low probability when  $P_1 \leq 0.5\%$ , middle probability when  $0.5\% < P_1 \leq 1\%$ , high probability when  $1\% < P_1 < 5\%$ , and extremely high probability when  $5\% \leq P_1$ . In another method of classification by Chang et al. (2017), debris flow intensity can be defined by maximum unit width discharge (Table 2), namely  $q$  ( $m^2/s$ ) defined as the maximum simulated flow depth ( $H$ ) multiplied by the maximum simulated velocity ( $V$ ), as well as the maximum simulated flow depth ( $H$ ) should be an important factor to be

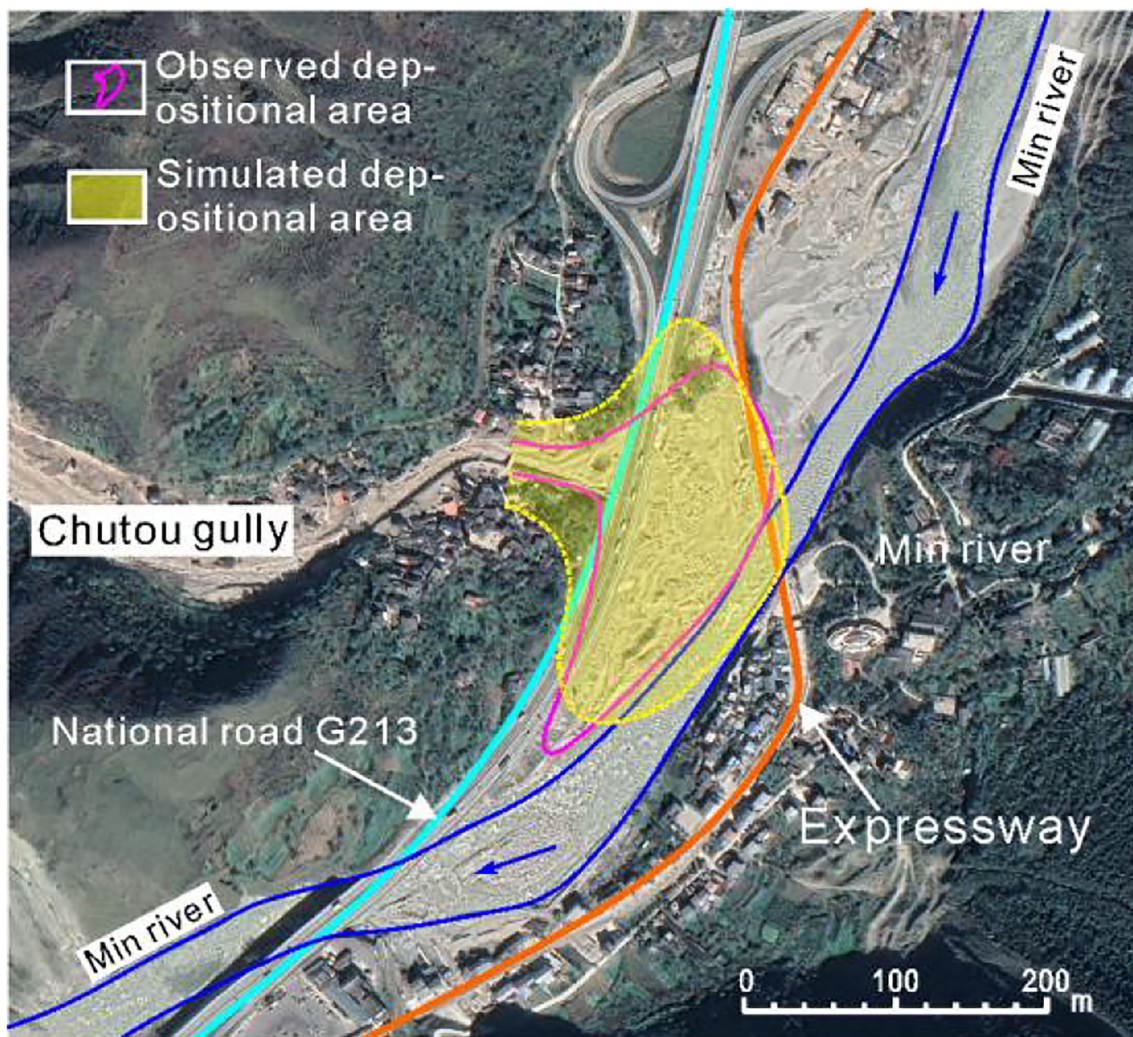


Fig. 13 Comparison of depositional area of Chutou gully between simulated and observed

considered. The movement process of Chutou gully was modeled with calibrated  $\mu = 0.225$  and  $\xi = 180m/s^2$ . Combining with intensity classification and occurrence

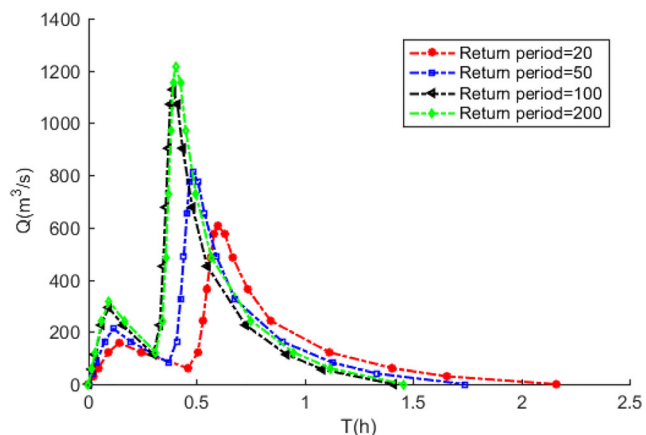


Fig. 14 Flow hydrograph of the Chutou gully debris flow for different return periods (20, 50, 100 and 200 years).

probability classification, debris flow hazard can be classified into low, middle and high degrees (Fig. 15).

Hazard map of Chutou gully under various rainfall return periods was formed, based on hazard classification standard stated above, through extracting the maximum flow depth and the maximum velocity from RAMMS software and inputting into GIS system (Fig. 16). The result showed that the affected area of debris flow increases with the increase of return period. In the future, this map can guide for land utilization planning and prevention and control designing in post-earthquake rebuilding area.

### Discussion and conclusion

This research applied RAMMS to simulate the dynamical development situation of the “8.20” Chutou gully post-earthquake debris flow and predict the hazard grade of it under different return period rainfall based on Vollemey-Salm fluid

**Table 2** Influential intensity of mud flow and debris flow

Debris flow intensity	Maximum simulated flow height H (m)	Relation	Maximum simulated flow height and velocity VH (m <sup>2</sup> /s)
Very high	$H > 3.0$	or	$VH > 12.0$
High	$1.5 < H \leq 3$	or	$3.0 < VH \leq 12.0$
Medium	$0.5 < H \leq 1.5$	and	$1.0 < VH \leq 3.0$
Low	$H < 0.5$	and	$VH < 1.0$

model. In the simulation results, the total volume of the material ran out of the gully mouth was larger than that of in-site observation, which may be due to the small initial discharge, part of the solid material rushing into the Min River was taken away by the turbulent water, and the solid material only could accumulate stably until the discharge was large enough. The total amount of solid material run out of the gully mouth is less than one-third of the total amount of material in the gully, and the rest is accumulated in the wide and gentle downstream of the gully. Therefore, this situation should be considered in the prevention of debris flow. Final flow depth of debris flow at each monitoring point is basically consistent with the field investigation, but it is slightly larger, especially in the upstream. The reason may be that during the investigation, some loose debris flow sediments in the gully were taken away by the perennial water in the gully.

Figure 14 shows that the larger the return period is, the larger the peak discharge is, and the shorter the time for the debris flow to reach the peak flow is. The hazard map of debris flow intensity and frequency (Fig. 16) shows that with the increase of debris flow return period, the larger the risk area of debris flow is, and the area of accumulation fan increased because of the increase of solid material run out of the gully mouth. Furthermore, the debris flow with a return period of 200 years may block the Min River.

RAMMS has two methods, block release and Input hydrograph, to set the initial conditions of debris flow. The

purpose is to calculate when the specific parameters of the source areas cannot be obtained (Frank et al. 2017). In the simulation, the calibration of Voellmy–Salm friction parameters with sufficient in-site investigation is the basis of numerical simulation and accurate prediction of Chutou gully. For the gully without debris flow in the near past, the friction parameters of adjacent gully can be used (Medina et al. 2008). DEM is an important factor affecting the accuracy of debris flow simulation, especially in depositional fan. The accuracy of DEM directly affects the terrain conditions of debris flow numerical simulation (Stolz and Huggel 2008). In the next research, we think that DEM with higher resolution is more suitable for numerical simulation of debris flow. At the same time, InSAR technology can help us to get the surface deformation data, so as to accurately determine the total amount of initiation solid material.

### Conclusion

According to numerical simulation and the experience of engineering construction in meizoseismal area (Chen et al. 2014), the reconstruction and prevention of post-earthquake debris flow should follow the following principles:

- The debris flow hazard areas at all stage should be avoided as much as possible.

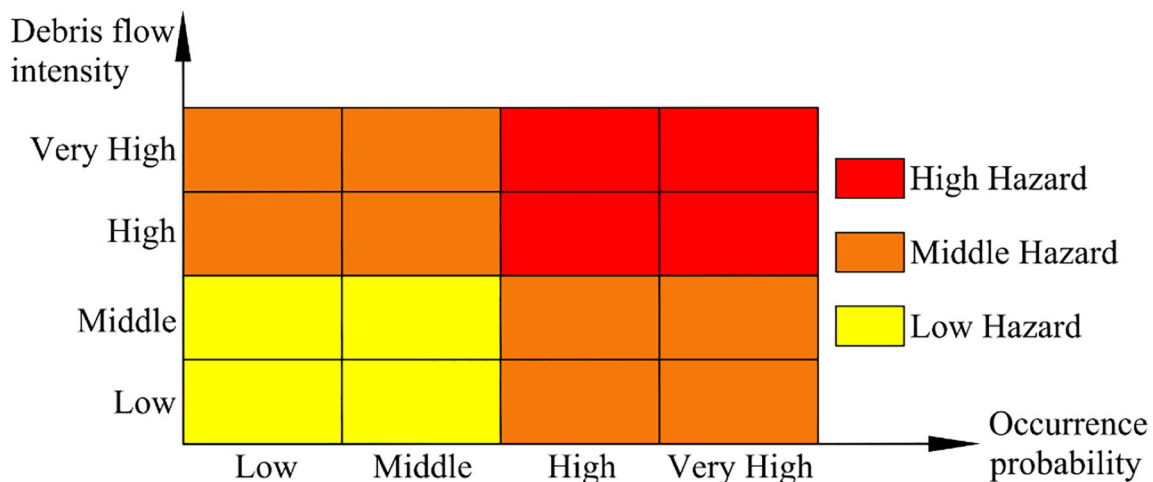


**Fig. 15** Classification of hazard in research zone

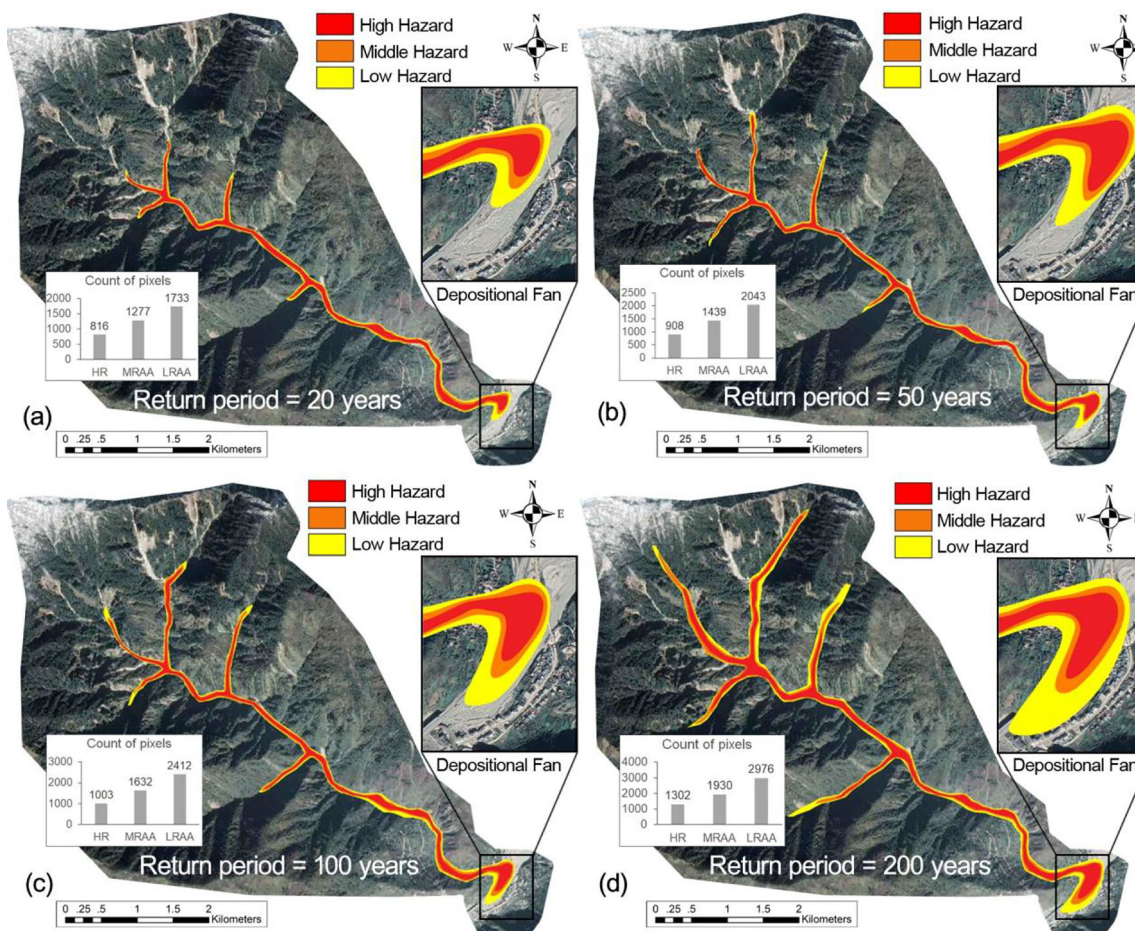


**Fig. 16** Debris flow intensity simulation for different return periods. **a** 20, **b** 50, **c** 100 and **d** 200 years. (HR is high hazard, MRAA is middle hazard and above and LRAA is low hazard and above)

- It is necessary to avoid building any kind of buildings in high hazard areas.
- Necessary protective engineering should be built when the project is constructed in the middle and low hazard areas. At the same time, it is necessary to avoid homes, schools, factories and other personnel intensive buildings being built-in middle hazard areas.
- Appropriate engineering measures (such as multi-stage dam) can be adopted to fix the material source in the gully to prevent the occurrence of debris flow or reduce its hazard.

Based on the content presented in this paper, the following conclusions was concluded:

1. Chutou gully is a typical post-earthquake debris flow induced by rainstorm. The triggering factor is that the accumulated rainfall exceeds the rainfall threshold in the study area. At the same time, the post-earthquake landslide accumulated in the gully provides enough solid materials for the outbreak of debris flow.
2. This research expounds the process of simulating debris flow by using RAMMS, which provides new ideas and methods for back calculation and hazard prediction of post-earthquake debris flow. The numerical simulation reappears the movement process of debris flow in Chutou gully from the aspects of flow depth, velocity and discharge, which is consistent with the field investigation. At the same time, the simulation results reveal that the Chutou gully is characterized by deposition upstream, and erosion downstream. The supply of the branch gully is the reason why the flow depth and velocity show many peaks. The simulation result shows that the maximum discharge of Chutou gully is  $955.52 \text{ m}^3/\text{s}$ , and the rainfall return period is about 50–100 years according to Fig. 14. The simulation results are helpful to understand the formation mechanism and development process of post-earthquake debris flow.
3. Based on the intensity and occurrence probability of debris flow, the debris flow hazard can be divided into high, middle and low degrees. Combined with numerical simulation and debris flow hazard classification standard, the



hazard prediction map of Chutou gully in various return periods (20, 50, 100 and 200 years) is constructed. The hazard map can provide information for the prediction and prevention of debris flow hazard in Chutou gully. In addition, the hazard classification model of post-earthquake debris flow can provide guidance for future land-use planning and debris flow prevention.

**Acknowledgments** Meanwhile, the authors would like to thank the two anonymous reviewers for their valuable comments, which significantly improved the manuscript.

**Funding** The authors would like to acknowledge the National key research and development program (2018YFC1505401), National Natural Science Foundation of China (41731285, 41672283), Youth Fund Project of NSFC (41907225) and Open fund of State Key Laboratory of geological disaster prevention and geological environment protection (SKLGP2018K011) for their strong support for this topic.

## Declarations

**Competing interests** The authors declare that they have no competing interests.

## References

- Bartelt, P., Bieler C., Bühler Y., Christen M., Deubelbeiss Y., Graf C., ... & Schneider, M. 2017. RAMMS: debris flow user manual. 15-16.
- Bartelt P, Salm B, Gruber U (1999) Calculating dense-snow avalanche runout using a Voellmy-fluid model with active/passive longitudinal straining. *J Glaciol* 45(150):242–254
- Bertolo P, & Bottino G (2008) Debris-flow event in the Frangerello stream-Susa valley (Italy)—calibration of numerical models for the back analysis of the 16 October, 2000 rainstorm. *landslides*, 5(1), 19-30.
- Chang FJ, Chiang YM, Lee WS (2009) Investigating the impact of the Chi-Chi earthquake on the occurrence of debris flows using artificial neural networks. *Hydrol Process* 23:2728–2736
- Christen M, Kowalski J, Bartelt P (2010) RAMMS: numerical simulation of dense snow avalanches in three-dimensional terrain. *Cold Reg Sci Technol* 63(1-2):1–14
- Chang M, Tang C, Van Asch TW, Cai F (2017) Hazard assessment of debris flows in the Wenchuan earthquake-stricken area, South West China. *Landslides* 14(5):1783–1792
- Chen X, Cui P, You Y, Chen J, Li D (2014) Engineering measures for debris flow hazard mitigation in the Wenchuan earthquake area. *Eng Geol* 194:73–85
- Crosta G (1998) Regionalization of rainfall thresholds: an aid to landslide hazard evaluation. *Environ Geol* 35(2-3):131–145
- Fan X, Scaringi G, Domènech G, Yang F, Guo X, Dai L et al (2019a) Two multi-temporal datasets that track the enhanced landsliding after the 2008 Wenchuan earthquake. *Earth Syst Sci Data* 11:35–55
- Fan X, Scaringi G, Korup O, West AJ, Van Westen CJ, Tanyas H et al (2019b) Earthquake-induced chains of geologic hazards: patterns, mechanisms, and impacts. *Rev Geophys* 57:421–503
- Fiebigger G (1997) Hazard mapping in Austria. *Journal of Torrent, Avalanche, Landslide and Rockfall Engineering* 61(134):121–133
- Frank F, McArdell BW, Oggier N, Baer P, Christen M, Vieli A (2017) Debris-flow modeling at Meretschibach and Bondasca catchments, Switzerland: sensitivity testing of field-data-based entrainment model. *Nat Hazards Earth Syst Sci* 17(5):801–815
- Gan J, Zhang YS (2019) Numerical simulation of debris flow runout using Ramms: a case study of Luzhuang Gully in China. *Comput Model Eng Sci*:981–1009
- Ge YG, Cui P, Zhang JQ, Zeng C, Su FH (2015) Catastrophic debris flows on July 10th 2013 along the Min River in areas seriously-hit by the Wenchuan earthquake. *J Mt Sci* 12:186–206
- Guo X, Cui P, Li Y, Fan J, Yan Y, Ge Y (2016) Temporal differentiation of rainfall thresholds for debris flows in Wenchuan earthquake-affected areas. *Environ Earth Sci* 75:109
- He K, Li Y, Ma G, Hu X, Liu B, Ma Z, Xu Z (2020) Failure mode analysis of post-seismic rockfall in shattered mountains exemplified by detailed investigation and numerical modelling. *Landslides*. <https://doi.org/10.1007/s10346-020-01532-1>
- He K, Ma G, Hu X, Liu B (2021) Failure mechanism and stability analysis of a reactivated landslide occurrence in Yanyuan City, China. *Landslides*. <https://doi.org/10.1007/s10346-020-01571-8>
- Horton AJ, Hales TC, Ouyang C, Fan X (2019) Identifying post-earthquake debris flow hazard using Massflow. *Eng Geol* 258: 105134
- Huang RQ, Li WL (2009) Analysis on the number and density of landslides triggered by the 2008 Wenchuan earthquake, China. *Journal of Geological Hazards and Environment Preservation* 20:1–7 (In Chinese)
- Huang X, Tang C, Zhou W (2014) Numerical simulation of occurrence frequency estimation model for debris flows. *J Eng Geol* 22(06): 1271–1278 (In Chinese)
- Hu W, Xu Q, Asch TV (2014) Experimental study on the initiation of debris flow. *Research & Applications, Unsaturated Soils*
- Li TT, Huang RQ, Pei XJ (2016) Variability in rainfall threshold for debris flow after Wenchuan earthquake in Gaochuan River watershed, Southwest China. *Natural Hazards* 82 (3):1967-1980
- Lin CW, Shieh CL, Yuan BD, Shieh YC, Liu SH, Lee SY (2004) Impact of Chi-Chi earthquake on the occurrence of landslides and debris flows: example from the Chenyulan River watershed, Nantou, Taiwan. *Eng Geol* 71:49–61
- Lin JY, Yang MD, Lin BR, Lin PS (2011) Risk assessment of debris flows in Songhe Stream, Taiwan. *Eng Geol* 123(1-2):100–112
- Luo G, Hu XW, Liang JX (2017) Stability evaluation and prediction of the Dongla reactivated ancient landslide as well as emergency mitigation for the Dongla Bridge. *Landslides* 14:1403–1418
- Ma C, Wang Y, Hu K, Du C, Yang W (2017) Rainfall intensity–duration threshold and erosion competence of debris flows in four areas affected by the 2008 Wenchuan earthquake. *Geomorphology* 282:85–95
- Medina V, Marcel H, Bateman A (2008) Application of FLAT-Model, a 2D finite volume code, to debris flows in the northeastern part of the Iberian Peninsula. *landslides* 5(1):127–142
- Minatti L, Pasculli A (2011) SPH numerical approach in modelling 2D muddy debris flow. In: *International Conference on Debris-Flow Hazards Mitigation: Mechanics, Prediction, and Assessment*, Proceedings, pp 467–475
- Naef D, Rickenmann D, Rutschmann P, McArdell BW (2006) Comparison of flow resistance relations for debris flows using a one-dimensional finite element simulation model. *Nat Hazards Earth Syst Sci* 6(1):155–165
- Pastor M, Blanc T, Haddad B, Petrone S, Sanchez Morles M, Drempetic V et al (2014) Application of a SPH depth-integrated model to landslide run-out analysis. *Landslides* 11(5):793–812
- Penserini BD, Roering JJ, Streig A (2017) A morphologic proxy for debris flow erosion with application to the earthquake deformation cycle, Cascadia Subduction Zone, USA. *Geomorphology* 282:150–161
- Prochaska AB, Santi PM, Higgins JD, Cannon SH (2008) A study of methods to estimate debris flow velocity. *Landslides* 5:431–444

- Pudasaini SP, & Hutter K (2007) *Avalanche dynamics: dynamics of rapid flows of dense granular avalanches*. Springer Science & Business Media.
- Rickenmann D, Laigle D, Mcardell BW, Hübl J (2006) Comparison of 2D debris-flow simulation models with field events. *Comput Geosci* 10(2):241–264
- Savage SB, Hutter K (1989) The motion of a finite mass of granular material down a rough incline. *J Fluid Mech* 199:177–215
- Shen YM, Chen TL, Xiao GJ et al (1984) Flood calculation manual of small watershed in Sichuan province. China. 15-17 (In Chinese)
- Stolz A, Huggel C (2008) Debris flows in the Swiss National Park: the influence of different flow models and varying DEM grid size on modeling results. *Landslides* 5(3):311–319
- Tang C, Zhu J, Ding J et al (2011) Catastrophic debris flows triggered by a 14 August 2010 rainfall at the epicenter of the Wenchuan earthquake. *Landslides* 8 (4):485-497
- Wang J, Yang S, Ou G, Gong Q, Yuan S (2018) Debris flow hazard assessment by combining numerical simulation and land utilization. *Bull Eng Geol Environ* 77(1):13–27
- Wu H, Jiang Y, Zhang X (2015) Flow models of fluidized granular masses with different basal resistance terms. *Geomechanics & Engineering* 8(6):811–828
- Yan Y, Cui YF, Yin SY (2020) Landslide reconstruction using seismic signal characteristics and numerical simulations: case study of the 2017 “6.24” Xinmo landslide [J]. *Eng Geol* 270:105582
- Zhang N, Takashi M, Ningbo P (2018) Numerical investigation of post-seismic debris flows in the epicentral area of the Wenchuan earthquake. *Bull Eng Geol Environ* 78:3253–3268